IEEE Access
Multidisciplinary ⋮ Rapid Review ⋮ Open Access Journal

Received July 14, 2021, accepted August 2, 2021, date of publication August 9, 2021, date of current version August 13, 2021.

Digital Object Identifier 10.1109/ACCESS.2021.3103321

Performance Analysis of Cognitive Radio Networks With Burst Dynamics

QIANYU XU[1], SUOPING LI[1,2], (Member, IEEE), TIEN VAN DO[3], (Member, IEEE), KEJUN JIA[4], AND NANA YANG[2]

[1]School of Electrical and Information Engineering, Lanzhou University of Technology, Lanzhou 730000, China
[2]School of Science, Lanzhou University of Technology, Lanzhou 730000, China
[3]Department of Networked Systems and Services, Budapest University of Technology and Economics, 1111 Budapest, Hungary
[4]School of Computer and Communications, Lanzhou University of Technology, Lanzhou 730000, China

Corresponding author: Suoping Li (lsuop@163.com)

This work was supported in part by the National Natural Science Foundation of China under Grant 61663024, in part by the Erasmus+ Programme under Grant 573879-EPP-1-2016-1-FR-EPPKA2-CBHE-JP, and in part by the Hongliu First Class Discipline Development Project of Lanzhou University of Technology, China.

ABSTRACT The impact of the traffic characteristics of secondary users (SUs) on the performance of cognitive radio networks (CRNs) should be understood for designing operation rules. This paper focuses on multi-type burst services and network congestion problem in CRNs and evaluates the QoS of SUs based on multiple cross-layer considerations. A two-state Markov-modulate Bernoulli process (MMBP-2) is adopted to model packet flows of SUs with different burst degrees in CRNs. We propose a two-dimensional discrete queuing model to consider spectrum access, burstiness of traffic, network congestion, channel environment, user activity and finite buffer. We construct an iterative algorithm to compute the steady-state distribution of the proposed queuing model and determine the performance metrics like the throughput, the average delay, the average queue length and the total packet loss probability. Numerical analysis evaluates the QoS of SUs under different burst environments.

INDEX TERMS Cognitive radio networks, burst traffic, network congestion, queuing model, two-dimensional Markov chain, performance evaluation.

I. INTRODUCTION

A. MOTIVATION

At present, the operation of the traditional wireless communication systems is based on the static licensed allocation of the radio spectrum. Research shows that the utilization of the licensed spectrum is low because licensed (primary) users are not always active on the allocated bands [1]. For the improvement of spectrum utilization [2], cognitive radio (CR) technology allows unlicensed (secondary) users to detect idle periods of the licensed spectrum and transmit data during periods when primary users (PUs) are not active [3], [4]. Sensing ability and reconfigurable ability are the necessary features of CR technology. Some licensed share access (LSA) concepts have been proposed to cope with unpredictable environments [5]–[7]. The performance evaluation of cognitive radio networks (CRNs) where the complex interaction between various factors (the burstiness of traffic, unpredictable environment, etc.) happens could help design operation rules.

The associate editor coordinating the review of this manuscript and approving it for publication was Ayaz Ahmad.

B. RELATED WORK

According to whether the PUs allow the SUs to coexist with them, CR is divided into three modes: interweave, overlay and underlay [8]. The research of this paper is mainly based on the overlay mode. In this mode, the SUs can excavate the spectrum hole of the PUs and communicate on the basis of guaranteeing the transmission performance of the PUs. In the overlay mode, the SUs satisfy their own services through cooperates with the PUs, in the form of renting the spectrum that the PUs do not often use or relaying the communication between the PUs. Chavez-Santiago *et al.* [9] proposed an ultra-wideband radio technology where the secondary systems can utilize the specific cognitive radio licensed bands to ensure reliable transmission. Researchers [5]–[7] investigated sharing rules where PUs cannot preempt the services of SUs during a predefined time interval, which protects the transmission of SUs.

TABLE 1. Summary of related references.

Ref.#	Cross-layer Consideration	Spectrum Sensing	Channel Fading	Multi-type SUs Traffic	Burst Traffic	Finite Buffer	Queuing Model	Focused Parameters	QoS Evaluation Indexes of SUs
2012 [11]	Yes	Yes	Yes	No	No	Yes	No	ARQ / AMC / Finite buffer size / Sensing errors / Rayleigh fading	Spectral efficiency / Power
2013 [12]	Yes	Yes	Yes	No	No	Yes	Yes	MAC protocol / ARQ / AMC / Finite buffer size / Sensing errors/ Block fading	Average queue length / Packet dropping rate / Packet collision rate
2016 [13]	Yes	Yes	Yes	No	No	Yes	Yes	ARQ / Finite buffer size / Sensing errors / Nakagami-m fading	Average delay / Packet lose rate
2017 [14]	Yes	Yes	No	No	No	No	Yes	ARQ / Sensing errors	Average delay / Throughput
2016 [15]	Yes	No	Yes	Yes	No	No	Yes	Priority of SUs / Infinite buffer / Gaussian noise	Average waiting time / Reneging probability / System idle probability
2018 [16]	No	No	No	Yes	No	No	Yes	Priority of SUs	Average waiting time / Number of user
2019 [17]	No	Yes	No	No	No	No	Yes	Interference quantity on PUs / Spectrum leasing cost	Throughput / blocking rate / Dropping rate / Interference quantity on the PUs
Proposed	Yes	Yes	Yes	Yes	Yes	Yes	Yes	Multi-type SUs traffic / Burst traffic / Congestion control / Finite buffer size / Nakagami-m fading	Average throughput / Average queue length / Average delay / Packet loss rate

Queuing model can describe the network model and analyze the system performance [10]. Therefore, it is an effective method to establish a queuing model to evaluate the performance of the secondary system in CRNs. Based on the cross-layer consideration, [11]–[14] investigated the access mode of the secondary system with the use of the queuing theory. Jian *et al.* [12] set up a discrete-time finite-state Markov chain to explore the impact of sensing errors, medium-access control (MAC) scheme, adaptive modulation and coding (AMC), automatic repeat-request (ARQ) and buffer size on the quality of service (QoS) of SUs. Simulation results [12] showed the influence of system settings on the QoS metrics of SUs. Furthermore, Zhang *et al.* [13] considered cross-layer factors such as path loss, ARQ and buffer capacity to establish the M/M/1/K queuing model to analyze the delay of SUs. Their results [13] indicated that the buffer capacity of SUs and the tolerable number of ARQ play an essential role in average delay and packet loss probability. Queuing models were established in [15], [16] to characterize the spectrum access mode of multi-priority SUs traffics, so as to evaluate the QoS. Yang *et al.* [17] established an objective function to obtain the optimal spectrum access strategy based on the interference quantity on PUs and the spectrum leasing cost. They applied a queuing model to evaluate the throughput of the secondary system. However, the above works did not consider the problem of multi-type burst services, especially the modeling and performance evaluation of SUs traffic with different burst degrees. Consequently, this motivates the investigation of our study, as observed in Table 1, which summarizes aspects considered by the literary works and shows what are new in this paper compared to the current results. This paper considers the physical layer and data link layer mechanism, traffic of multi-type burst, congestion control based on the random early detection (RED) [18] algorithm to evaluate the QoS of SUs. In addition, we also take the channel model at the physical layer into consideration.

By considering the listed parameters, multi-type burst services are modeled and analyzed. Since data traffic bursts at any time scale, there exists a certain correlation between traffics with different burst degrees. Autocorrelation is used to describe burstiness. The two-state Markov-modulate Bernoulli process (MMBP-2) model differentiates an input source into two states, then the correlation between them can be established with the Markov chain [19].

C. NOVELTY AND CONTRIBUTIONS

In this paper, through studying the spectrum access mode of multi-type SUs services with different burst degrees, we consider multiple cross-layer factors that affect spectrum access including channel environment, user activity, multi-type burst services, finite buffer and network congestion. The above factors are integrated into a two-dimensional probability space and a two-dimensional stochastic process is proposed to describe the system. The main contributions of this paper are as follows:

1) *A model integrates multi-factors and cross-layer considerations.* This paper integrates multiple affecting factors of spectrum access, such as multi-type burst services, network congestion, channel environment,

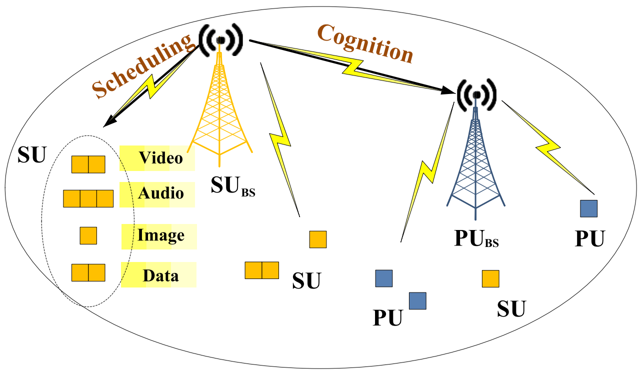

FIGURE 1. Cognitive radio network model.

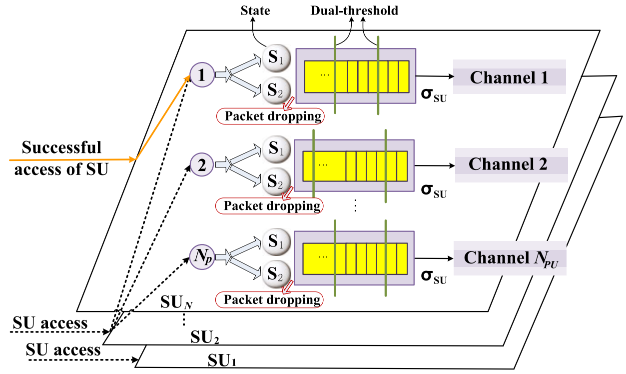

FIGURE 2. The spectrum access mode of burst services.

user activity and finite buffer. The traffics generated by SUs belong to one of two types, and the MMBP-2 process models their bursty nature. The proposed model also considers the congestion control performed by the dual-threshold RED algorithm. To our best knowledge, no such model is available so far.

2) *Construct a two-dimensional Markov chain.* A two-dimensional Markov chain is constructed to integrate the above mentioned affecting factors into a two-dimensional probability space. Then, a mathematical model is used to solve the performance evaluation problem.
3) *Design of iterative algorithm:* An iterative algorithm is presented to compute the steady-state probabilities of the two-dimensional Markov chain and the performance metrics (throughput, average delay, average queue length and total packet loss probability).
4) Congestion control management approaches (no congestion control, dynamic random early detection, and random early detection) are compared. The impact of channel fading on the system performance is investigated.

II. QUEUING MODEL

A. ASSUMPTIONS

We consider a CRN system that operates in discrete-time slots. A clustered time-slot CRN model with a finite number of PUs and SUs is illustrated in Figure 1. The information transmitted through CR may be of multiple types, including data, image, audio and video. The SUs are heterogeneous, independent and identically distributed (i.i.d). Each cluster has one base station for PUs (PU_{BS}) and one for SUs (SU_{BS}). The direction of data transmission considered in this paper is the uplink from SU_{BS} to PU_{BS}. According to the past channel observation, the probability of a channel idle in the next slot is estimated. The scheduling of the SUs is performed by the SU_{BS} based on the spectrum estimation results. At each time slot, the cognitive phase and the transmission phase may happen. If PU does not occupy the channel at the beginning of a specific slot, the PU will not use the channel throughout the slot.

In this paper, we make further assumptions as well:

1) Control node can perform orderly scheduling for multi-type SUs traffics, and then the collision between SUs can be avoided.
2) PUs and SUs apply the overlay mode of a predefined resource sharing rule where the PUs cannot preempt the services of the SUs within a predefined time interval [5].
3) The SU packets enter the channel according to the First Come First Service (FCFS) principle.

As shown in Figure 2, a buffer with finite capacity (K) is set for SUs at SU_{BS}. Let N_{PU} and SU_{N} be the number of PUs and SUs, respectively.

In CRNs, SUs may transmit packets carrying either data/image or audio/video. These traffics are mostly burst and usually has a certain correlation between traffics with different burst degrees. In data link layer, this paper adopts MMBP-2 as the input source model to characterize the queuing dynamic of traffics with different burst degrees. MMBP-2 consists of two states to differentiate traffics with different burst degrees. Markov chain can be used to link the transitions between the states to depict the correlation between the different type of packets. The data/image service has a short frame length and high delay tolerance, while the audio/video service has a low tolerance for delay. Therefore, traffics of a specific bursty degree in the data link layer are described by the discrete-time, Markov-modulated Bernoulli process (MMBP-2) with two states (S_1 and S_2), where S_1 represent the state of a particular SU when it transmits an audio/video packet while S_2 corresponds to the SU's state when it sends a data/image traffic.

Since burst traffics likely cause congestion, a dual-threshold queue management scheme named random early detection (RED) is adopted for the SUs queuing in the buffer, where the congestion of secondary network is controlled by actively dropping a small part of data packets.

SU packets leaving the buffer will enter the channel and begin the service. A SU can access any idle channel, and the sum of the probabilities of accessing all the idle channels is 1. A channel corresponds to a server in the queuing model. In what follows, we only describe the internal user activity

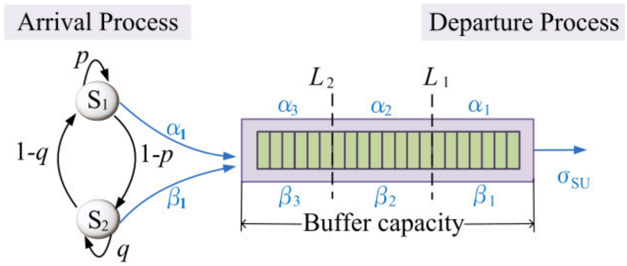

FIGURE 3. Queuing process.

of one of the channels, so the established queuing model has a single server. Assume that the Nakagami fading model describes the characteristic of a channel in the physical layer. Not that the probability that the specific data packet of SUs is successful received on the channel is affected by the propagation link, the activity of PUs and the cognitive ability of SUs. Therefore, the channel fading and the user activity jointly determine the successful reception probability, σ_{SU}, of SUs.

If the arrival of the SU traffic is in state S_1 (S_2) in the current slot, the probability of remaining in S_1 (S_2) in the next slot is p (q), and the probability of transferring to state S_2 (S_1) is $1-p$ $(1-q)$. The process obeys the Bernoulli distribution and the rate of sending a packet in states S_1 and S_2 are α_1 and β_1, respectively.

The MMBP-2 process is characterized by the transition probability matrix P and the arrival rate matrix Λ_1 as:

$$P = \begin{bmatrix} p & 1-p \\ 1-q & q \end{bmatrix} = \begin{bmatrix} p & \bar{p} \\ \bar{q} & q \end{bmatrix}, \ \Lambda_1 = \begin{bmatrix} \alpha_1 & 0 \\ 0 & \beta_1 \end{bmatrix} \tag{1}$$

The MMBP-2 process has the following characteristics [19].

1) The average arrival rate:

$$\rho = (\bar{q}\alpha_1 + \bar{p}\beta_1)/(\bar{p}+\bar{q}) \tag{2}$$

2) The squared coefficient of variation of the interarrival time, c^2, describes the burst degree of SUs traffic as:

$$c^2 = \frac{2\rho[(\bar{p}+\bar{q})^2 + (\bar{p}\alpha_1 + \bar{q}\beta_1)(p+q-1)]}{(\bar{p}+\bar{q})[\bar{q}\alpha_1 + \bar{p}\beta_1 + \alpha_1\beta_1(p+q-1)]} - \rho - 1 \tag{3}$$

3) The first-order autocorrelation coefficient of the inter-arrival time, $\phi(1)$, and the x-th order auto-correlation coefficient of the number of SU's arrivals based on MMBP-2, $\Phi(x)$, which describes the correlation between the arrivals of SUs traffic as:

$$\varphi(1) = \frac{\alpha_1\beta_1(\alpha_1-\beta_1)^2\bar{p}\bar{q}(p+q-1)^2}{c^2(\bar{p}+\bar{q})^2[\bar{q}\alpha_1+\bar{p}\beta_1+\alpha_1\beta_1(p+q-1)]^2} \tag{4}$$

$$\Phi(x) = \frac{\bar{p}\bar{q}(\alpha_1-\beta_1)^2(p+q-1)^x}{(\bar{q}\alpha_1+\bar{p}\beta_1)[\bar{q}(1-\alpha_1)+\bar{p}(1-\beta_1)]} \tag{5}$$

A buffer with the finite capacity, K, is set for SUs at each terminal in SU_{BS}. There are SU_N secondary users. We assume that SU_{BS} applies a control mechanism with L_1 and L_2 thresholds, $0 < L_1 < L_2 < K$, (see Figure 3).

Upon the arrival of a packet,

1) if the queue length is less than L_1, the packet is stored in the buffer;
2) if the queue length is between L_1 and L_2, and the arrival process is in state S_1, the packet is dropped with probability $1-\alpha_2$;
3) if the queue length is between L_1 and L_2, and the arrival process is in state S_2, the packet is dropped with probability $1-\beta_2$;
4) if the queue length exceeds L_2, and the arrival process is in state , it is dropped with probability $1-\alpha_3$;
5) if the queue length exceeds L_2, and the arrival process is in state S_2, it is dropped with probability $1-\beta_3$.

Note that $\alpha_3 < \alpha_1$, $\beta_3 < \beta_1$, the values of α_m and $\beta_m (m = 1,\ 2,\ 3.)$ are set as:

$$\alpha_m = \begin{cases} \alpha_1, & 0 \le j < L_1 \\ \alpha_1 + \dfrac{(\alpha_3-\alpha_1)(j-L_1+1)}{L_2-L_1+1}, & L_1 \le j < L_2 \\ \alpha_3, & L_1 \le j \le K; \end{cases}$$
$$\beta_m = \begin{cases} \beta_1 & 0 \le j < L_1 \\ \beta_1 + \dfrac{(\beta_3-\beta_1)(j-L_1+1)}{L_2-L_1+1}, & L_1 \le j < L_2 \\ \beta_3, & L_1 \le j \le K \end{cases}. \tag{6}$$

where j, $(0 \le j \le K,\ j \in Z)$ is the current length of the SUs queue.

Let σ_{SU} denotes the probability that the data packet of SUs is successful received on channel. Assume that radio propagation link between any pair of nodes generated in the transmission process in the transmission process is affected by the independent stationary Nakagami flat-fading channel, and the envelope of the received signal is r_{SU}. SUs can always perform correct spectrum sensing. Thus, the probability that the SU packet is successfully received when only SU exists in channel, $P_{\{SUsucc|SU\}}$, can be obtained:

$$\begin{aligned} P_{\{SUsucc|SU\}} &= \Pr\left\{ |r_{SU}(t)|^2 > \frac{C_{SU}R_{SU}}{P_{SU}} \right\} \\ &= \Gamma(m_{SU}, \frac{m_{SU}C_{SU}R_{SU}}{P_{SU}})/\Gamma(m_{SU}) \end{aligned} \tag{7}$$

where $\Gamma(n) = (n-1)!$, $\Gamma(n,x) = (n-1)!e^{-x}\sum_{j=0}^{n-1} x^j/j!$. R_{SU} and m_{SU} are the path loss and the Nakagami fading parameter of SU propagation link, P_{SU} and C_{SU} are the transmission power and the receiver signal-noise ratio (SNR) of the SU.

The successful reception probability of SUs is also affected by the activity of PUs. PUs also have their physical queues at each terminal. According to the spectrum resource sharing rule assumed in this paper, the physical queue length of PU is 0 (i.e., $L_{PU} = 0$) when only the SU transmits data in the channel. As a consequence, the successful reception probability of SUs is:

$$\sigma_{SU} = \Pr\{L_{PU} = 0\} \cdot P_{\{SUsucc|SU\}} \cdot (1-P_f) \tag{8}$$

where P_f is the false alarm probability. Since the probability of $L_{PU} = 0$ is 1, then we obtained:

$$\sigma_{SU} = P_{\{SUsucc|SU\}} \cdot (1-P_f) \tag{9}$$

In addition, [13] also discusses the probability that the SUs being received successfully with sensing errors. Since the focus of this study is to evaluate the service performance of secondary system without considering the collision between packets, the situation of sensing errors will not repeat here.

B. QUEUING ANALYSIS

Let j represents the current queue length of SUs in the buffer. A two-dimensional Markov chain $\{(s, j),\ s = 1,\ 2;\ j = 0,\ 1,\ 2,\ \ldots, L_1-1,\ L_1, \ldots,\ L_2,\ L_2+1, \ldots, K\}$ is used to describe the system. The transition diagram of the Markov chain is depicted in Figure 4.

The probability that the queue length is j at the current slot, and it will not change at the next slot is $P^R_{s,j\to s,j}$. Let $P^A_{s,j\to s,j+1}$ denote the probability that the current queue length is j and it changes to $j+1$ at the next slot. Let $P^D_{s,j\to s,j-1}$ be the probability that the current queue length is j and it goes to $j-1$ at the next slot. The rise in the queue length indicates that a data packet enters the SU queue, while the decrease is due to the departure of a packet after completing the service.

The probability that the sending rate is α_m and the queue length is j at the current slot while the sending rate changes to β_m and the queue length changes to $j-1$ at the next slot is $P^D_{1,j\to 2,j-1}$. The probability that the sending rate is β_m and the queue length is j at the current slot, then the sending rate changes to α_m and the queue length is $j-1$ at the next slot is $P^D_{2,j\to 1,j-1}$. $P^D_{1,j\to 1,j-1}$ or $P^D_{2,j\to 2,j-1}$ represents the probability that the sending rate is $\alpha_m(\beta_m)$, the queue length is j and the queue length changes to $j-1$ at the next slot but the sending rate is not change. Thus, the transition probabilities of two-dimensional Markov chain which consist of $P^D_{s,j\to s,j-1} P^A_{s,j\to s,j+1}$ and $P^R_{s,j\to s,j}$ are as follows:

1) The probability, $P^D_{s,j\to s,j-1}$, $(1 \le j \le K)$, of a packet departure at the next slot is:

$$P^D_{1,j\to 1,j-1} = \begin{cases} (1-\alpha_1)\sigma_{SU}p, & 1 \le j \le L_1 \\ (1-\alpha_2)\sigma_{SU}p, & L_1 < j \le L_2 \\ (1-\alpha_3)\sigma_{SU}p, & L_2 < j \le K; \end{cases}$$

$$P^D_{1,j\to 2,j-1} = \begin{cases} \sigma_{SU}(1-\alpha_1)(1-p), & 1 \le j \le L_1 \\ \sigma_{SU}(1-\alpha_2)(1-p), & L_1 < j \le L_2 \\ \sigma_{SU}(1-\alpha_3)(1-p), & L_2 < j \le K \end{cases}$$

$$P^D_{2,j\to 2,j-1} = \begin{cases} (1-\beta_1)\sigma_{SU}q, & 1 \le j \le L_1 \\ (1-\beta_2)\sigma_{SU}q, & L_1 < j \le L_2 \\ (1-\beta_3)\sigma_{SU}q, & L_2 < j \le K; \end{cases}$$

$$P^D_{2,j\to 1,j-1} = \begin{cases} \sigma_{SU}(1-\beta_1)(1-q), & 1 \le j \le L_1 \\ \sigma_{SU}(1-\beta_2)(1-q), & L_1 < j \le L_2 \\ \sigma_{SU}(1-\beta_3)(1-q), & L_2 < j \le K. \end{cases} \tag{10}$$

2) The probability, $P^A_{s,j\to s,j+1}$, $(0 \le j < K)$, of a packet arrival at the next slot is:

$$P^A_{1,j\to 1,j+1} = \begin{cases} \alpha_1 p, & j = 0 \\ \alpha_1 p(1-\sigma_{SU}), & 1 \le j < L_1 \\ \alpha_2 p(1-\sigma_{SU}), & L_1 \le j < L_2 \\ \alpha_3 p(1-\sigma_{SU}), & L_2 \le j < K; \end{cases}$$

$$P^A_{1,j\to 2,j+1} = \begin{cases} \alpha_1(1-p), & j = 0 \\ \alpha_1(1-\sigma_{SU})(1-p), & 1 \le j < L_1 \\ \alpha_2(1-\sigma_{SU})(1-p), & L_1 \le j < L_2 \\ \alpha_3(1-\sigma_{SU})(1-p), & L_2 \le j < K; \end{cases}$$

$$P^A_{2,j\to 2,j+1} = \begin{cases} \beta_1 q, & j = 0 \\ \beta_1 q(1-\sigma_{SU}), & 1 \le j < L_1 \\ \beta_2 q(1-\sigma_{SU}), & L_1 \le j < L_2 \\ \beta_3 q(1-\sigma_{SU}), & L_2 \le j < K; \end{cases}$$

$$P^A_{2,j\to 1,j+1} = \begin{cases} \beta_1(1-q), & j = 0 \\ \beta_1(1-\sigma_{SU})(1-q), & 1 \le j < L_1 \\ \beta_2(1-\sigma_{SU})(1-q), & L_1 \le j < L_2 \\ \beta_3(1-\sigma_{SU})(1-q), & L_2 \le j < K \end{cases} \tag{11}$$

3) The probability, $P^R_{s,j\to s,j}$, $(0 \le j \le K)$, that the packet still in its original queue length state at the next slot is:

$$P^R_{1,j\to 1,j} = \begin{cases} (1-\alpha_1)p, & j = 0 \\ [\alpha_1\sigma_{SU}+(1-\alpha_1)(1-\sigma_{SU})]p, & 1 \le j < L_1 \\ [\alpha_2\sigma_{SU}+(1-\alpha_2)(1-\sigma_{SU})]p, & L_1 \le j < L_2 \\ [\alpha_3\sigma_{SU}+(1-\alpha_3)(1-\sigma_{SU})]p, & L_2 \le j < K \\ [\alpha_3+(1-\alpha_3)(1-\sigma_{SU})]p, & j = K; \end{cases}$$

$$P^R_{1,j\to 2,j} = \begin{cases} (1-\alpha_1)(1-p), & j = 0 \\ [\alpha_1\sigma_{SU}+(1-\alpha_1)(1-\sigma_{SU})](1-p), & 1 \le j < L_1 \\ [\alpha_2\sigma_{SU}+(1-\alpha_2)(1-\sigma_{SU})](1-p), & L_1 \le j < L_2 \\ [\alpha_3\sigma_{SU}+(1-\alpha_3)(1-\sigma_{SU})](1-p), & L_2 \le j < K \\ [\alpha_3+(1-\alpha_3)(1-\sigma_{SU})](1-p), & j = K \end{cases}$$

$$P^R_{2,j\to 2,j} = \begin{cases} (1-\beta_1)q, & j = 0 \\ [\beta_1\sigma_{SU}+(1-\beta_1)(1-\sigma_{SU})]q, & 1 \le j < L_1 \\ [\beta_2\sigma_{SU}+(1-\beta_2)(1-\sigma_{SU})]q, & L_1 \le j < L_2 \\ [\beta_3\sigma_{SU}+(1-\beta_3)(1-\sigma_{SU})]q, & L_2 \le j < K \\ [\beta_3+(1-\beta_3)(1-\sigma_{SU})]q, & j = K; \end{cases}$$

$$P^R_{2,j\to 1,j} = \begin{cases} (1-\beta_1)(1-q), & j = 0 \\ [\beta_1\sigma_{SU}+(1-\beta_1)(1-\sigma_{SU})](1-q), & 1 \le j < L_1 \\ [\beta_2\sigma_{SU}+(1-\beta_2)(1-\sigma_{SU})](1-q), & L_1 \le j < L_2 \\ [\beta_3\sigma_{SU}+(1-\beta_3)(1-\sigma_{SU})](1-q), & L_2 \le j < K \\ [\beta_3+(1-\beta_3)(1-\sigma_{SU})](1-q), & j = K \end{cases} \tag{12}$$

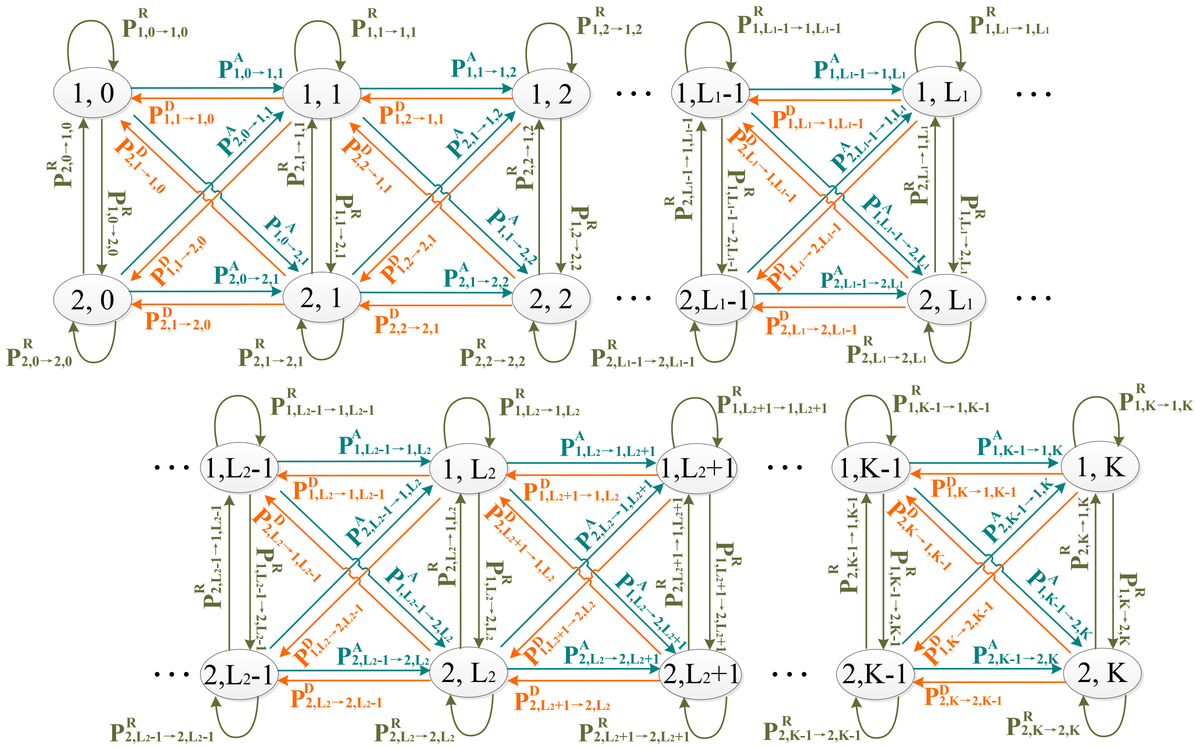

FIGURE 4. Two-dimensional state transition process with MMBP-2 as input source.

Note that there are two possible scenarios when the queue length remains unchanged in the last case above: i) either the number of arrival and departure packets cancels each other out, or ii) there is no arrival and departure packet in the SU queue. When the first scenario occurs, a packet has been served successfully. Otherwise, the packet is not served successfully. In particular, when the SU queue is empty, no packet can be served. When it is full, the probability that the packet being successfully served is 1.

Let $\pi(s, j)$ be the steady-state probability of state $(s,\ j)$, $(0 \le j \le K,\ \ s = 1\ or\ s = 2)$. Then the balance equations of the two-dimensional Markov chain are as follows (13), as shown at the bottom of the next page.

Let $\Lambda_m = \begin{pmatrix} \alpha_m & 0 \\ 0 & \beta_m \end{pmatrix}$, $(m = 1,\ 2,\ 3)$, $P = \begin{bmatrix} p & 1-p \\ 1-q & q \end{bmatrix}$, and arrange the states in (13) in lexicographic order, combining with (10)-(12), the transition probability of two-dimensional Markov chain with the finite state space can be expressed as matrix Q where (14), as shown at the bottom of the next page, where F_1', E_1', D_m, E_m, F_m, E_3, as shown at the bottom of the next page.

Let $\pi_j = \pi(1,\ j)+\pi(2,\ j)$ represents the steady-state probability of the queue length j, $(j = 0,\ 1,\ 2,\ \ldots,\ K)$. Therefore, equation (13) can be transformed into the following form:

$$\pi Q = \pi \text{ and } \pi e = 1,\ \text{where } e = [1,\ 1,\ 1,\ \ldots,\ 1]^T_{(K+1)\times 1} \tag{15}$$

where $\pi = [\pi_0,\ \pi_1,\ \pi_2,\ \ldots,\ \pi_K]$ is the steady-state distribution of the system model.

C. CALCULATION OF THE STEADY-STATE DISTRIBUTION

Following [20], an iterative algorithm is constructed to solve (14) for steady-state distribution. To ease the comprehension, we present steps for $L_1 = 4,\ L_2 = 11,\ K = 15$. In this case, matrix Q can be expressed as Q, as shown at the bottom of the page 110634.

Note that Q is a matrix of size 32×32 and composed of block matrices of size 2×2.

The idea is to reduce the block matrix with size 16×16 to a one-block matrix with size 1×1 in the forward reduction phase. After getting the steady-state solution of one-block matrix (named boundary vector), the solution is expanded layer by layer to obtain the steady-state solution of matrix Q in the backward expansion phase. The layer here is the row of Q, and the number of the layers corresponds to the current queue length of the SU queue, j, in the buffer. The details of our algorithm are as follows:

1) FORWARD REDUCTION PHASE

Firstly, permute the rows and columns of the blocks of layer 0-15 of matrix Q in the following order:

$$\begin{pmatrix} 0 & 1 & 2 & 3 & 4 & 5 & 6 & 7 & 8 & 9 & 10 & 11 & 12 & 13 & 14 & 15 \\ 0 & 2 & 4 & 6 & 8 & 10 & 12 & 14 & 1 & 3 & 5 & 7 & 9 & 11 & 13 & 15 \end{pmatrix}.$$

That is, the blocks of Q in layer 1 goes to the place of layer 2, layer 2 goes to the place of layer 4, etc. As a result,

$$
\begin{cases}
\pi(1,\ 0) = P^R_{1,0\to 1,0}\pi(1,\ 0)+P^R_{2,0\to 1,0}\pi(2,\ 0)+P^D_{2,1\to 1,0}\pi(2,\ 1)+P^D_{1,1\to 1,0}\pi(1,\ 1) \\
\pi(1,\ 1) = P^R_{1,1\to 1,1}\pi(1,\ 1)+P^R_{2,1\to 1,1}\pi(2,\ 1)+P^A_{1,0\to 1,1}\pi(1,\ 0)+P^A_{2,0\to 1,1}\pi(2,\ 0) \\
\quad +P^D_{2,2\to 1,1}\pi(2,\ 2)+P^D_{1,2\to 1,1}\pi(1,\ 2) \\
\quad \cdots\cdots \\
\pi(1,\ K-1) = P^R_{1,K-1\to 1,K-1}\pi(1,\ K-1)+P^R_{2,K-1\to 1,K-1}\pi(2,\ K-1) \\
\quad +P^A_{1,K-2\to 1,K-1}\pi(1,\ K-2)+P^A_{2,K-2\to 1,K-1}\pi(2,\ K-2) \\
\quad +P^D_{2,K\to 1,K-1}\pi(2,\ K)+P^D_{1,K\to 1,K-1}\pi(1,\ K) \\
\pi(1,\ K) = P^R_{1,K\to 1,K}\pi(1,\ K)+P^R_{2,K\to 1,K}\pi(2,\ K)+P^A_{1,K-1\to 1,K}\pi(1,\ K-1) \\
\quad +P^A_{2,K-1\to 1,K}\pi(2,\ K-1) \\
\pi(2,\ 0) = P^R_{2,0\to 2,0}\pi(2,\ 0)+P^R_{1,0\to 2,0}\pi(1,\ 0)+P^D_{2,1\to 2,0}\pi(2,\ 1)+P^D_{1,1\to 2,0}\pi(1,\ 1) \\
\pi(2,\ 1) = P^R_{2,1\to 2,1}\pi(2,\ 1)+P^R_{1,1\to 2,1}\pi(1,\ 1)+P^A_{2,0\to 2,1}\pi(2,\ 0)+P^A_{1,0\to 2,1}\pi(1,\ 0) \\
\quad +P^D_{2,2\to 2,1}\pi(2,\ 2)+P^D_{1,2\to 2,1}\pi(1,\ 2) \\
\quad \cdots\cdots \\
\pi(2,\ K-1) = P^R_{2,K-1\to 2,K-1}\pi(2,\ K-1)+P^R_{1,K-1\to 2,K-1}\pi(1,\ K-1) \\
\quad +P^A_{2,K-2\to 2,K-1}\pi(2,\ K-2)\ +P^A_{1,K-2\to 2,K-1}\pi(1,\ K-2) \\
\quad +P^D_{2,K\to 2,K-1}\pi(2,\ K)+P^D_{1,K\to 2,K-1}\pi(1,\ K) \\
\pi(2,\ K) = P^R_{2,K\to 2,K}\pi(2,\ K)+P^R_{1,K\to 2,K}\pi(1,\ K)+P^A_{1,K-1\to 2,K}\pi(1,\ K-1) \\
\quad +P^A_{2,K-1\to 2,K}\pi(2,\ K-1).
\end{cases}
\tag{13}
$$

$$
Q_{2(K+1)\times 2(K+1)} =
\begin{array}{c}
\begin{array}{cccccccccccccc}
0 & 1 & \ldots & L_1-1 & L_1 & L_1+1 & \ldots & L_2-1 & L_2 & L_2+1 & \ldots & K-1 & K
\end{array} \\
\begin{pmatrix}
E_1' & F_1' & & & & & & & & & & & \\
D_1 & E_1 & F_1 & & & & & & & & & & \\
 & \cdots & \cdots & \cdots & & & & & & & & & \\
 & & D_1 & E_1 & F_1 & & & & & & & & \\
 & & & D_2 & E_2 & F_2 & & & & & & & \\
 & & & & D_2 & E_2 & F_2 & & & & & & \\
 & & & & & \cdots & \cdots & \cdots & & & & & \\
 & & & & & & D_2 & E_2 & F_2 & & & & \\
 & & & & & & & D_3 & E_3 & F_3 & & & \\
 & & & & & & & & D_3 & E_3 & F_3 & & \\
 & & & & & & & & \cdots & \cdots & \cdots & & \\
 & & & & & & & & & D_3 & E_3 & F_3 & \\
 & & & & & & & & & & D_3 & E_3' &
\end{pmatrix}
\end{array}
\begin{array}{c} \\ 0 \\ 1 \\ \cdots \\ L_1-1 \\ L_1 \\ L_1+1 \\ \cdots \\ L_2-1 \\ L_2 \\ L_2+1 \\ \cdots \\ K-1 \\ K \end{array}
\tag{14}
$$

$$
\begin{aligned}
F_1 &= \begin{pmatrix} \alpha_1 p & \alpha_1(1-p) \\ \beta_1(1-q) & \beta_1 q \end{pmatrix} = \Lambda_1 P; \\
E_1' &= \begin{pmatrix} (1-\alpha_1)p & (1-\alpha_1)(1-p) \\ (1-\beta_1)(1-q) & (1-\beta_1)q \end{pmatrix} = (I-\Lambda_1)P; \\
D_m &= \begin{pmatrix} \sigma_{SU}(1-\alpha_m)p & \sigma_{SU}(1-\alpha_m)(1-p) \\ \sigma_{SU}(1-\beta_m)(1-q) & \sigma_{SU}(1-\beta_m)q \end{pmatrix} \\
&= \sigma_{SU}(I-\Lambda_m)P; \\
E_m &= \begin{pmatrix} [\alpha_m\sigma_{SU}+(1-\alpha_m)(1-\sigma_{SU})]p & [\alpha_m\sigma_{SU}+(1-\alpha_m)(1-\sigma_{SU})](1-p) \\ [\beta_m\sigma_{SU}+(1-\beta_m)(1-\sigma_{SU})](1-q) & [\beta_m\sigma_{SU}+(1-\beta_m)(1-\sigma_{SU})]q \end{pmatrix} \\
&= \Lambda_m\sigma_{SU}P+(I-\Lambda_m)(1-\sigma_{SU})P; \\
F_m &= \begin{pmatrix} (1-\sigma_{SU})\alpha_m p & (1-\sigma_{SU})\alpha_m(1-p) \\ (1-\sigma_{SU})\beta_m(1-q) & (1-\sigma_{SU})\beta_m q \end{pmatrix} = (1-\sigma_{SU})\Lambda_m P; \\
E_3' &= \begin{pmatrix} [\alpha_3+(1-\alpha_3)(1-\sigma_{SU})]p & [\alpha_3+(1-\alpha_3)(1-\sigma_{SU})](1-p) \\ [\beta_3+(1-\beta_3)(1-\sigma_{SU})](1-q) & [\beta_3+(1-\beta_3)(1-\sigma_{SU})]q \end{pmatrix} = \Lambda_3 P+(I-\Lambda_3)(1-\sigma_{SU})P.
\end{aligned}
$$

the original order [0, 1, 2, 3, 4, 5, 6, 7, 8, 9, 10, 11, 12, 13, 14, 15] is updated to [0, 2, 4, 6, 8, 10, 12, 1, 3, 5, 7, 9, 11, 13, 15], and we obtained matrix Q_0;

Next, divide Q_0 into two groups (group S and group T) with four parts according to the layer. Reduce Q_0 to half the size of the original block matrix according to $Q_1 = Q_t^{(0)} + Q_{ts}^{(0)}(-Q_s^{(0)})^{-1} Q_{st}^{(0)}$. The resulting submatrix Q_1 inherits the matrix form of Q_0. The reduced Q_1 is a new parent matrix Q_0, as shown at the bottom of the page.

Then, permute the layer of the new parent matrix as shown in Figure 5. Repeat the above reduction steps 1-2 until the

$$Q = \begin{pmatrix}
E_1' & F_1' \\
D_1 & E_1 & F_1 \\
& D_1 & E_1 & F_1 \\
&& D_1 & E_1 & F_1 \\
&&& D_2 & E_2 & F_2 \\
&&&& D_2 & E_2 & F_2 \\
&&&&& D_2 & E_2 & F_2 \\
&&&&&& D_2 & E_2 & F_2 \\
&&&&&&& D_2 & E_2 & F_2 \\
&&&&&&&& D_2 & E_2 & F_2 \\
&&&&&&&&& D_2 & E_2 & F_2 \\
&&&&&&&&&& D_2 & E_2 & F_2 \\
&&&&&&&&&&& D_3 & E_3 & F_3 \\
&&&&&&&&&&&& D_3 & E_3 & F_3 \\
&&&&&&&&&&&&& D_3 & E_3 & F_3 \\
&&&&&&&&&&&&&& D_3 & E_3'
\end{pmatrix}.$$

$$Q_0 = \begin{pmatrix}
E_1' & F_1' \\
D_1 & E_1 & F_1 \\
& D_2 & E_2 & F_2 \\
&& D_2 & E_2 & F_2 \\
&&& D_2 & E_2 & F_2 \\
&&&& D_2 & E_2 & F_2 \\
&&&&& D_3 & E_3 & F_3 \\
&&&&&& D_3 & E_3 & F_3 \\
&&&&&&& D_1 & E_1 & F_1 \\
&&&&&&&& D_1 & E_1 & F_1 \\
&&&&&&&&& D_2 & E_2 & F_2 \\
&&&&&&&&&& D_2 & E_2 & F_2 \\
&&&&&&&&&&& D_2 & E_2 & F_2 \\
&&&&&&&&&&&& D_2 & E_2 & F_2 \\
&&&&&&&&&&&&& D_3 & E_3 & F_3 \\
&&&&&&&&&&&&&& D_3 & E_3'
\end{pmatrix}$$

$$\to \left(\begin{array}{cccccccc|cccccccc}
E_1' &&&&&&&& F_1' \\
& E_1 &&&&&&& D_1 & F_1 \\
&& E_2 &&&&&&& D_2 & F_2 \\
&&& E_2 &&&&&&& D_2 & F_2 \\
&&&& E_2 &&&&&&& D_2 & F_2 \\
&&&&& E_2 &&&&&&& D_2 & F_2 \\
&&&&&& E_3 &&&&&&& D_3 & F_3 \\
&&&&&&& E_3 &&&&&&& D_3 & F_3 \\
\hline
D_1 & F_1 &&&&&&& E_1 \\
& D_1 & F_1 &&&&&&& E_1 \\
&& D_2 & F_2 &&&&&&& E_2 \\
&&& D_2 & F_2 &&&&&&& E_2 \\
&&&& D_2 & F_2 &&&&&&& E_2 \\
&&&&& D_2 & F_2 &&&&&&& E_2 \\
&&&&&& D_3 & F_3 &&&&&&& E_3 \\
&&&&&&& D_3 &&&&&&&& E_3'
\end{array}\right)$$

$$= \begin{pmatrix} Q_s^{(0)} & Q_{st}^{(0)} \\ Q_{ts}^{(0)} & Q_t^{(0)} \end{pmatrix}$$

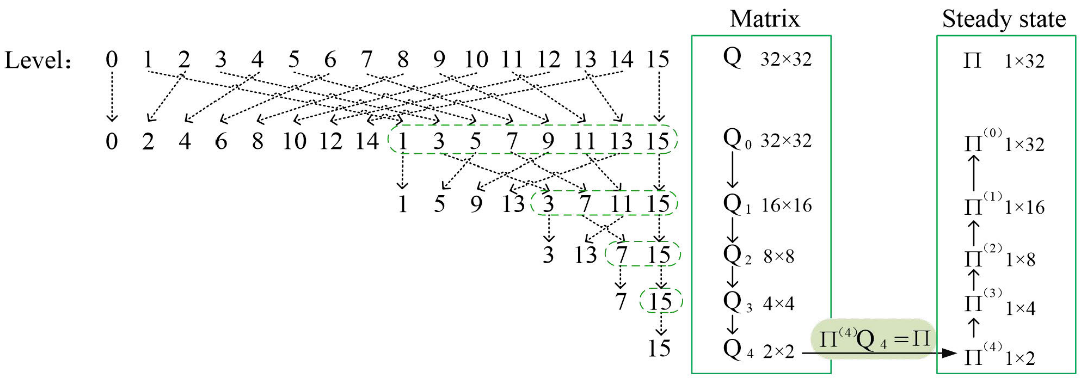

FIGURE 5. Level reduction process.

original block matrix Q_0 is reduced to a one-block matrix Q_4: $Q_0 \to Q_1 \to Q_2 \to Q_3 \to Q_4$;

2) BOUNDARY VECTOR OBTAINING PHASE

Obtain the boundary solution vector $\pi^{(4)}$ according to $\pi^{(4)}Q_4 = \pi$;

3) BACKWARD EXPANSION PHASE

The solution vector of Q_3 can be obtained from $\pi^{(3)} = \pi^{(4)} \cdot [-Q_{ts}^{(3)} Q_s^{(3)-1},\ I]$, where I is the identity matrix. After finite iterations $\pi^{(4)} \to \pi^{(3)} \to \pi^{(2)} \to \pi^{(1)} \to \pi^{(0)}$, $\pi^{(0)} = \pi^{(1)} \cdot [-Q_{ts}^{(0)} Q_s^{(0)-1},\ I]$ can be obtained.

Following the reverse order in Figure 5 as:

$$\begin{pmatrix} 0 & 2 & 4 & 6 & 8 & 10 & 12 & 14 & 1 & 3 & 5 & 7 & 9 & 11 & 13 & 15 \\ 0 & 1 & 2 & 3 & 4 & 5 & 6 & 7 & 8 & 9 & 10 & 11 & 12 & 13 & 14 & 15 \end{pmatrix},$$

the blocks of $\pi^{(0)}$ in layer 2 return back to the place of layer 1, layer 4 return back to the place of layer 2. The order of the steady-state $\pi^{(0)}$, $[0,\ 2,\ 4,\ 6,\ 8,\ 10,\ 12,\ 14,\ 1,\ 3,\ 5,\ 7,\ 9,\ 11,\ 13,\ 15]$ is updated to $[0,\ 1,\ 2,\ 3,\ 4,\ 5,\ 6,\ 7,\ 8,\ 9,\ 10,\ 11,\ 12,\ 13,\ 14,\ 15]$.

Finally, the matrix π after layer updating is the steady-state distribution of matrix Q with size 1×32.

Note that a computational method in [21] can also be applied as well to determine the steady-state distribution.

D. PERFORMANCE MEASURES

Based on the stationary distribution, the following system performance metrics can be determined.

1) The average queue length, $E(L)$, is:

$$E(L) = \sum\nolimits_{\mathrm{j}=0}^{\mathrm{K}} j\,[\pi(1,\ j)+\pi(2,\ j)] \tag{16}$$

2) The average throughput, $E(S)$, is the number of packets successfully transmitted by the secondary system per unit time (packets/slot) as:

$$E(S) = P_{SU}(1-P_f)[1-\pi(1,\ 0)-\pi(2,\ 0)] \tag{17}$$

TABLE 2. Arrival rate of different traffics.

Index		α_1	β_1	ρ	c^2	ϕ	Φ
STRONG	1	0.55	0.0004	0.5	50	0.1	0.1
	2	0.60	0.0007	0.5	100	0.2	0.2
	3	0.65	0.0009	0.5	150	0.3	0.3
	4	0.70	0.0011	0.5	200	0.4	0.4
	5	0.75	0.0013	0.5	250	0.5	0.5
	6	0.80	0.0015	0.5	300	0.6	0.6
	7	0.85	0.0017	0.5	350	0.7	0.7
WEAK	8	0.90	0.0018	0.5	400	0.8	0.8

3) Average delay, $E(W)$, is determined by the Little's Law:

$$E(W) = \frac{E(L)}{E(S)} = \frac{\sum_{j=0}^{K} j[\pi(1,j)+\pi(2,j)]}{\sigma_{SU}[1-\pi(1,\ 0)-\pi(2,\ 0)]} \tag{18}$$

4) Packet loss probability of the secondary system, D_{pl}, is:

$$D_{pl} = [\pi(1,K)+\pi(2,K)][1-P_{SU}(1-P_f)] \tag{19}$$

III. NUMERICAL RESULTS

In this section, three study cases are carried out with parameters as $R_{SU} = 5$, $m_{SU} = 1$, $P_{SU} = 20$, $C_{SU} = 6$, $P_f = 0.05$, $K = 15$.

A. IMPACT OF CONGESTION CONTROL ON SECONDARY SYSTEM PERFORMANC

We compare three congestion control schemes: RED, no congestion control (NCC) and dynamic random early detection (DRED). The difference between RED and DRED is the number of thresholds. RED adopts dual-threshold control ($L_1 = 3$, $L_2 = 12$ are used for the study), while DRED uses a single threshold ($L = 12$ for the study).

Table 2 contains the parameters $(\alpha_1, \beta_1, \rho,\ c^2,\ \phi,\ \Phi)$ of the arrival process for the numerical study. The index represents the bursty degree of the arrival process. The higher the index is, the heavier the traffic places the load on the system.

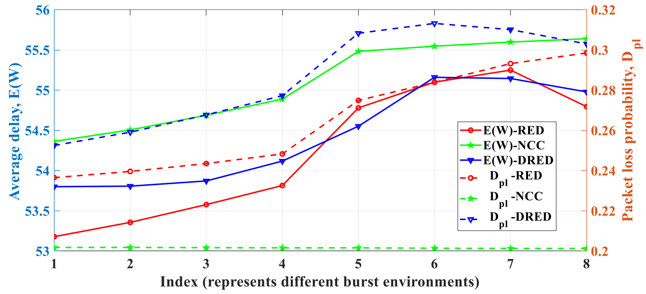

FIGURE 6. Effect of congestion control mechanism on the QoS of SUs.

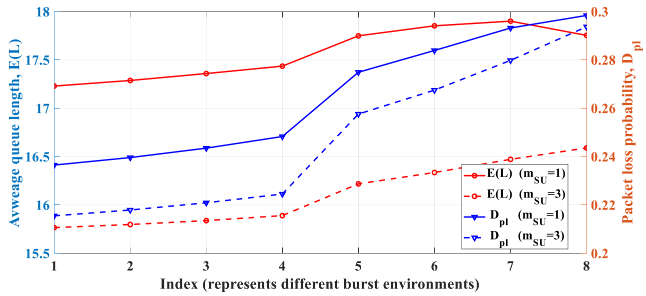

FIGURE 7. Effect of Nakagami fading on the QoS of SUs.

In Figure 6, we plot the average delay and the packet loss probability versus the index for three congestion control schemes. It can be observed that when the index value increases, the value of $E(W)$ and D_{pl} will also increase. Since RED and DRED drop a small number of packets to prevent the queue overflow. Therefore, the system with NCC has lower D_{pl} than with RED or DRED. However, as can be seen from Figure 6, the secondary network has higher $E(W)$. As we know, $E(L)$ is in proportion to $E(W)$, that is, the QoS of SUs with NCC environment is obviously low.

Although the packet loss probability of RED and DRED is higher, the difference value does not exceed 0.1 compared with the NCC environment, which is still acceptable. When the index value is between 4 and 6, the packet loss probability and the average delay increase significantly with the RED/DRED mechanism. When it exceeds 6, the growth slope slows down. That is, congestion mechanisms effectively cope with the bursty traffic to improve the performance of the secondary system. Furthermore, RED achieves a lower delay and packet loss probability than DRED.

B. IMPACT OF CHANNEL FADING ON SECONDARY SYSTEM PERFORMANCE

This section investigates the impact of the Nakagami fading channel. Figure 7 plots the average queue length and the packet loss probability versus the index and the parameter, m_{SU}, of the Nakagami fading channel. Note that the smaller m_{SU} represents the severe fading of the propagation link, the worse the channel state is.

From Figure 7, we can observe that the average queue length and the packet loss probability are more significant in the network environment with more bursty traffic. Moreover, the severe fading leads to higher $E(L)$ and D_{pl}.

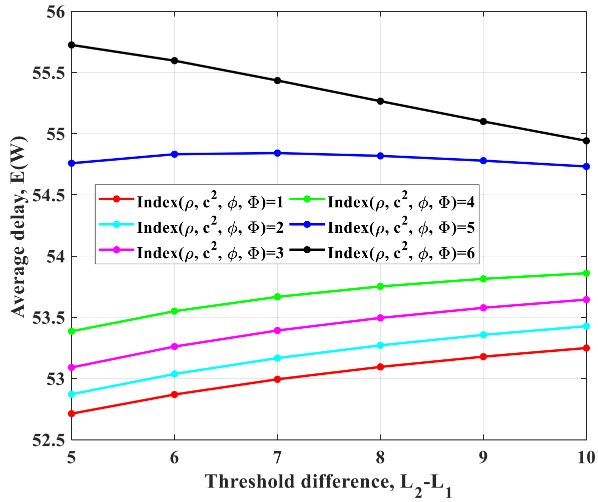

FIGURE 8. Average delay vs. Threshold difference.

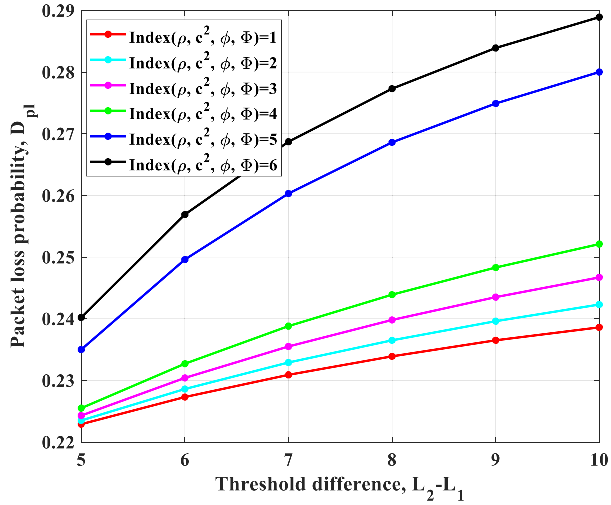

FIGURE 9. Packet loss probability vs. Threshold difference.

Results show that the channel fading in physical layer has a great influence on secondary system. In CRNs, the transmission quality of SUs is indeed affected by the channel environment, and the fading parameter focused on this paper is necessary for the evaluation of secondary network performance.

C. PERFORMANCE ANALYSIS OF SECONDARY SYSTEM

This section explores the overall performance of secondary system in network environments with different burst degrees by adjusting dual-threshold in queue management. Let us fix $L_1 = 3$, and adjust L_2, we discuss how to control and optimize system parameters to improve the overall performance. Threshold difference $L_2 - L_1$ represents the smooth interval of congestion control. Figures 8 and 9 show the comparison of the average delay and packet loss probability versus the setting of $(\rho,\ c^2,\ \phi,\ \Phi)$ and $L_2 - L_1$. The value of the statistics $(\rho,\ c^2,\ \phi,\ \Phi)$ are also presented in Table 2.

As observed from Figure 8, the increase of $L_2 - L_1$ decreases the average delay due to the traffic with a high

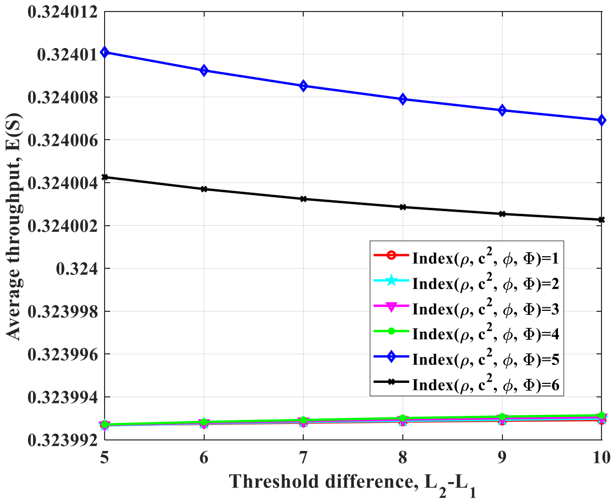

FIGURE 10. Average throughput vs. Threshold difference.

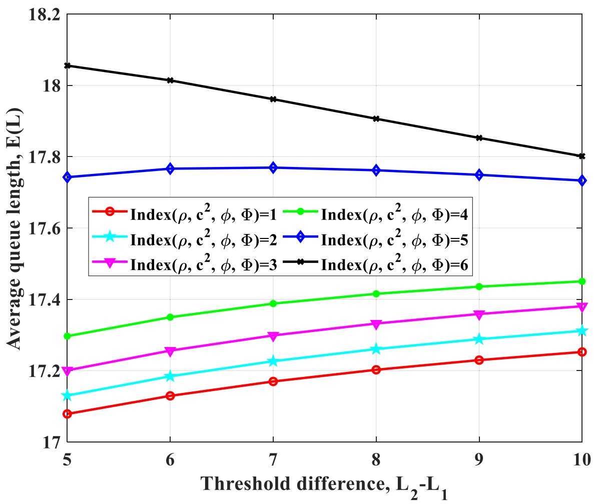

FIGURE 11. Average queue length vs. Threshold difference.

bursty degree. However, the average delay decrease comes with a high packet loss probability (see Figure 9). It is worth mentioning that the increasing packet loss probability is still within tolerance. With the increase of $L_2 - L_1$, RED has a more chance to alleviate the instantaneous congestion before the queue length grows too large. From Figure 9, it can be observed that the proper setting of $L_2 - L_1$ helps the stable operation of the system.

Figures 10 and 11 show the average throughput and average queue length versus $L_2 - L_1$ and burst degree. As shown in Figure 10, under the influence of channel environment and burst traffic, the results show that the system throughput fluctuates around 0.324. Compared with the model established in the general environment, the throughput in burst environment is relatively low. This is because when burst traffic arrives, the system may violate the normal service rules due to the late service. Furthermore, the proposed model can maintain the stable throughput under the network environment with serious burstiness.

In addition, Figure 11 shows that the average queue length and the average delay have similar trends. It is not difficult to find in Little's law that the average queue length varies directly as the average delay. Thus, the stable throughput makes similar graph trends of the queue length and delay.

Secondary network performance shows a downward trend when the more serious burst occurs. However, properly increasing the smooth interval of RED can control the deterioration of system performance by dropping little packets in advance. The access model with MMBP-2 as the input source established in this paper can maintain the stability of the QoS of SUs in complex environments. Moreover, in CRNs with multi-type services, different types of traffics have different QoS requirements. Real-time audio/video services are more sensitive to delay, while non-real-time services have lower delay requirements. The model parameters can be set according to actual transmission environment.

IV. CONCLUSION

We have presented a queuing model to evaluate the impact of bursty traffic in CRNs. SUs traffic sending audio/video services and data/image services can be modeled as the MMBP-2 process. Our model considers the RED congestion control, Nakagami fading channel. We have also constructed an iterative algorithm to obtain the steady-state solution and the performance metrics such as throughput, average queue length, queuing delay and packet loss probability. Extensive numerical results have been performed to investigate the impact of various parameters on the system. We have shown that RED with the dual-threshold could alleviate the deterioration of bursty traffic to improve network QoS. The research parameters in this paper provides a novel idea for performance analysis of CRNs with burstiness.

REFERENCES

[1] V. Kiruthika and S. Vembu, "Dynamic handover algorithm with interference cancellation in 5G networks for emergency communication," *Int. J. Commun. Syst.*, vol. 33, no. 5, pp. 1–19, Dec. 2019.

[2] A. Trotta, M. Di Felice, L. Bedogni, L. Bononi, and F. Panzieri, "Connectivity recovery in post-disaster scenarios through cognitive radio swarms," *Comput. Netw.*, vol. 91, pp. 68–89, Nov. 2015.

[3] D. Wang, B. Song, D. Chen, and X. Du, "Intelligent cognitive radio in 5G: AI-based hierarchical cognitive cellular networks," *IEEE Wireless Commun.*, vol. 26, no. 3, pp. 54–61, Jun. 2019.

[4] *Second Memorandum Opinion and Order in the Matter of Unlicensed Operation in the TV Broadcast Bands (ET Docket No. 04-186) and Additional Spectrum for Unlicensed Devices Below 900 MHz and in the 3 GHz Band (ET Docket No. 02-380)*, FCC, Washington, DC, USA, 2010.

[5] I. A. M. Balapuwaduge, F. Y. Li, and V. Pla, "Dynamic spectrum reservation for CR networks in the presence of channel failures: Channel allocation and reliability analysis," *IEEE Trans. Wireless Commun.*, vol. 17, no. 2, pp. 882–898, Feb. 2018.

[6] A. Chouayakh, A. Bechler, I. Amigo, L. Nuaymi, and P. Maillé, "Auction mechanisms for licensed shared access: Reserve prices and revenue-fairness trade offs," *ACM SIGMETRICS Perform. Eval. Rev.*, vol. 46, no. 3, pp. 43–48, Jan. 2019.

[7] E. Markova, I. Gudkova, A. Ometov, I. Dzantiev, S. Andreev, and Y. Koucheryavy, "Flexible spectrum management in a smart city within licensed shared access framework," *IEEE Access*, vol. 5, pp. 22252–22261, Oct. 2017.

[8] H. M. Karaca, "Throughput maximization of multichannel allocation mechanism under interference constraint for hybrid overlay/underlay cognitive radio networks with energy harvesting," *Wireless Netw.*, vol. 26, no. 6, pp. 3905–3928, Aug. 2020.

[9] R. Chávez-Santiago, K. E. Nolan, O. Holland, L. D. Nardis, and I. Balasingham, "Cognitive radio for medical body area networks using ultra-wideband," *IEEE Wireless Commun.*, vol. 19, no. 4, pp. 74–81, Aug. 2012.
[10] S. Li, F. Wang, J. Gaber, and X. Chang, "Throughput and energy efficiency of cooperative ARQ strategies for VANETs based on hybrid vehicle communication mode," *IEEE Access*, vol. 8, pp. 114287–114304, Jun. 2020.
[11] F. T. Foukalas, G. T. Karetsos, and L. F. Merakos, "Cross-layer design in opportunistic spectrum access-based cognitive radio networks," *Int. J. Commun. Netw. Distrib. Syst.*, vol. 8, nos. 3–4, pp. 230–246, Apr. 2012.
[12] J. Wang, A. Huang, L. Cai, and W. Wang, "On the queue dynamics of multiuser multichannel cognitive radio networks," *IEEE Trans. Veh. Technol.*, vol. 62, no. 3, pp. 1314–1328, Mar. 2013.
[13] L. Zhang, T. Song, J. Hu, and X. Bao, "Analysis of spectrum access strategy with multiple cross-layer considerations in cognitive radio networks," *Wireless Pers. Commun.*, vol. 87, no. 4, pp. 1383–1400, Sep. 2016.
[14] J. D. Kim and G. Hwang, "Cross-layer modeling and optimization of multi-channel cognitive radio networks under imperfect channel sensing," *J. Ind. Manage. Optim.*, vol. 11, no. 3, pp. 807–828, Oct. 2017.
[15] L. Chen, L. Huang, H. Xu, and Y. Du, "Queueing analysis for preemptive transmission in underlay CRNs," *Int. J. Commun. Syst.*, vol. 29, no. 6, pp. 1138–1155, Apr. 2016.
[16] S. E. Saad, I. F. Tarrad, and A. A. Ammar, "Spectrum access queuing based scheme for prioritised cognitive radio networks," *Int. J. Wireless Mobile Comput.*, vol. 15, no. 4, pp. 351–358, 2018.
[17] Y. Yang, Q. Zhang, Y. Wang, T. Emoto, M. Akutagawa, and S. Konaka, "Multi-strategy dynamic spectrum access in cognitive radio networks: Modeling, analysis and optimization," *China Commun.*, vol. 16, no. 3, pp. 103–121, Mar. 2019.
[18] S. Li, Q. Xu, J. Gaber, Z. Dou, and J. Chen, "Congestion control mechanism based on dual threshold DI-RED for WSNs," *Wireless Pers. Commun.*, vol. 115, no. 3, pp. 2171–2195, Dec. 2020.
[19] A. Alsaaidah, M. Zalisham, M. Fadzli, and H. Abdel-Jaber, "Markov-modulated Bernoulli-based performance analysis for gentle BLUE and BLUE algorithms under bursty and correlated traffic," *J. Comput. Sci.*, vol. 12, no. 6, pp. 289–299, Jun. 2016.
[20] J. D. Ye and S. Q. Li, "Folding algorithm: A computational method for finite QBD processes with level-dependent transitions," *IEEE Trans. Commun.*, vol. 42, nos. 2–4, pp. 625–639, Feb./Mar./Apr. 1994.
[21] T. V. Do, N. H. Do, and R. Chakka, "A new queueing model for spectrum renting in mobile cellular networks," *Comput. Commun.*, vol. 35, no. 10, pp. 1165–1171, Jun. 2012.

QIANYU XU received the B.S. degree in applied mathematics from Jiangsu Ocean University (formerly Huaihai Institute of Technology), China, in 2014. She is currently pursuing the Ph.D. degree in control theory and control engineering with Lanzhou University of Technology, China. Her research interests include stochastic modeling analysis of wireless communication networks, wireless sensor networks, and cognitive radio networks.

SUOPING LI (Member, IEEE) received the B.Sc. degree in mathematics from Northwest Normal University, in 1986, the M.Sc. degree in stochastic model with applications from Lanzhou University, in 1996, and the Ph.D. degree in signal and information processing from Beijing Jiaotong University, China, in 2004. He was a Visiting Scholar with the Swiss Federal Institute of Technology Zurich (ETH), from May 2007 to May 2008, and also a Visiting Professor with American East Texas Baptist University (ETBU), from August to December 2011. He completed short academic visits at Universite de Technologie Belfort-Montbeliard (UTBM) France, in 2017, and at Università degli Studi dell'Aquila (UNIVAQ), Italy, in 2018. He is currently a Full Professor with the School of Science, Lanzhou University of Technology (LUT), China. His research interests include stochastic modeling analysis of wireless communication networks, performance evaluation and planning of data communication protocol, applied stochastic process, and stochastic control.

TIEN VAN DO (Member, IEEE) received the M.Sc. and Ph.D. degrees in telecommunications engineering from the Technical University of Budapest, Hungary, in 1991 and 1996, respectively, and the D.Sc. degree from the Hungarian Academy of Sciences, in 2011. He is currently a Professor with the Department of Networked Systems and Services, Budapest University of Technology and Economics. He habilitated at BME. He led various projects on network planning and software implementations that results are directly used for industry such ATM & IP network planning software with Hungarian Telekom, GGSN tester for Nokia, performance testing program for the performance testing of the NOKIA's IMS product, automatic software testing framework with Nokia Siemens Networks. His research interests include queuing theory, telecommunication networks, cloud computing, performance evaluation and planning of ICT systems, and machine learning.

KEJUN JIA received the M.S. degree in communication and information system from Xi'an University of Technology, Xi'an, China, in 2007, and the Ph.D. degree in communication and information system from Southwest Jiaotong University, Chengdu, China, in 2018. Since 2001, he has been with the School of Computer and Communication, Lanzhou University of Technology, Lanzhou, China, where he is currently a Full Professor. His research interests include indoor visible light communications, multi-carrier systems as well as the next-generation wireless communications.

NANA YANG received the B.S. degree in mathematics from the Beifang University of Nationalities, Yinchuan, China, in 2007, and the M.S. and Ph.D. degrees in operational research and cybernetics from Xidian University, Xi'an, China, in 2010 and 2020, respectively. She is currently a Lecturer with the School of Science, Lanzhou University of Technology, Lanzhou, China. Her research interests include learning control of MASs and adaptive control.